Improving Coagulation Kinetics: A Mathematical Approach to Incorporating Intermediate Complexes in Thrombin Models

Alexandra Whiteside[†] and Emily Phan [‡]
Project advisor: Dr. Karin Leiderman, PhD [§]

Abstract. Hemostasis is a vital physiological process that prevents excessive bleeding through a cascade of complex biochemical reactions, resulting in blood clot formation. This process involves a coagulation cascade that converts fibrinogen to fibrin by thrombin. Mathematical models, including the Hockin-Mann, Danforth, and Lakshmanan models, have been instrumental in simulating thrombin generation and understanding the coagulation cascade. However, these models often use simplified reaction schemes and neglect the inclusion of intermediate complexes, which can compromise their accuracy. This study demonstrates that such simplifications distort the time scale and peak values of thrombin generation, leading to misleading results. By modifying all three mathematical models to incorporate classical enzyme kinetics and critical intermediate steps, we show that the modifications change the dynamics of thrombin generation and emphasize the need for a more detailed representation of the biochemical interactions involved. This work underscores the importance of employing comprehensive modeling approaches in coagulation studies to achieve a more accurate representation of thrombotic and hemophilic conditions, ultimately aiding in the development of effective therapeutic strategies.

1. Introduction. Hemostasis is an innate response that stops bleeding when there is an injury to the blood vessel. Hemostasis consists of two components: primary hemostasis, in which platelets accumulate and activate at the site of injury, and secondary hemostasis, in which coagulation reinforces and stabilizes the "platelet plug" by depositing a fibrin mesh network [15]. The process of blood clot formation is shown in Figure 1. A crucial part of this process is coagulation, a multi-reaction cascade that ultimately converts fibrinogen to fibrin, forming the structural basis of a stable blood clot.

Alterations in hemostatic balance can lead to thrombotic diseases or hemophilia. A better understanding of the coagulation process would permit the kinetics of these diseases to be better understood. Computational modeling can quantify reaction details of complex systems such as coagulation in order to predict experimental conditions and aid laboratory experiments. Mathematical models are particularly valuable because they can simulate intricate interactions between clotting factors, including the end product thrombin, under varying conditions. This approach allows models to investigate scenarios that would be difficult or costly to replicate in a lab setting, such as rare genetic variations or extreme physiological states. Mathematical modeling also provides insight into the nonlinear dynamics of clot formation and dissolution, making it easier to identify key regulatory points in the cascade. These models can be used to test potential interventions, evaluate drug efficacy, and even predict patient-specific responses to therapies, ultimately contributing to more precise and effective treatments for thrombin-related disorders.

[†]Department of Mathematics, University of North Carolina at Chapel Hill (alexandrawhiteside@alumni.unc.edu)

[‡]Department of Mathematics, University of North Carolina at Chapel Hill (ephan@unc.edu)

[§] Departments of Mathematics & Biochemistry and Biophysics, University of North Carolina at Chapel Hill (karinlg@unc.edu)

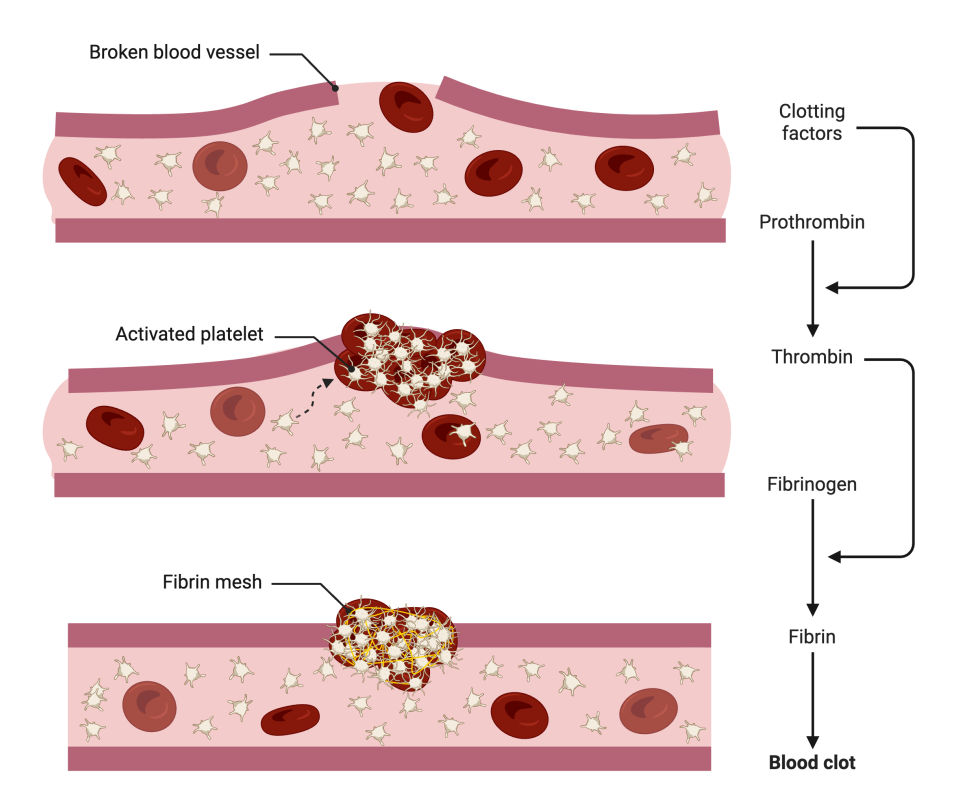


Figure 1: Overview of blood clot formation. The flowchart on the right shows this coagulation process in which clotting factors generate the fibrin mesh labeled on the bottom panel. Platelets, fibrin, and red blood cells accumulate at the injury site, forming a plug that stops bleeding. Created with BioRender.com.

1.1. Biological Background. The coagulation cascade includes enzymes, zymogens (inactive enzymes), and protein cofactors, which are represented by Roman numerals. Many of the reactions are enzyme-substrate reactions that result in the conversion of zymogens to their active enzyme components. The activated zymogens are indicated by adding the suffix "a" to each factor (for example, factor Xa is the activated factor X). Coagulation consists of the extrinsic pathway initiated by tissue factor and the intrinsic pathway (contact pathway) initiated by factor XII [15].

The extrinsic pathway of coagulation begins when an injury to endothelial tissue occurs, exposing the transmembrane protein tissue factor (TF) to the blood [15]. Tissue factor, a high-affinity receptor and cofactor for factors VII and VIIa, binds factor VIIa, which is preexistent in plasma after being synthesized in the liver [5]. The two proteins form the TF:VIIa complex, which acts as the primary driver for the extrinsic pathway. The TF:VIIa complex, in turn, activates factor IX to factor IXa and factor X to factor Xa [8]. Two other complexes play key roles in coagulation: the tenase complex (VIIIa:IXa) and the prothrombinase complex

(Xa:Va). In these complexes, cofactors VIIIa and Va greatly enhance the catalytic efficiency of enzymes IXa and Xa, respectively, compared to the enzymes alone [13]. The tenase complex activates factor X to factor Xa, while the prothrombinase complex activates prothrombin (factor II) to thrombin (factor IIa) [3]. Thrombin is considered the "end product" as it cleaves fibrinogen (factor I) to fibrin (factor Ia), forming a fibrin mesh over the clot [3]. Most experiments measure thrombin concentration over time as an indicator of blood clot formation progression. Thrombin also activates platelets and factors V, VIII, and XI, amplifying the cascade through positive feedback [3]. These reactions are summarized in Figure 2.

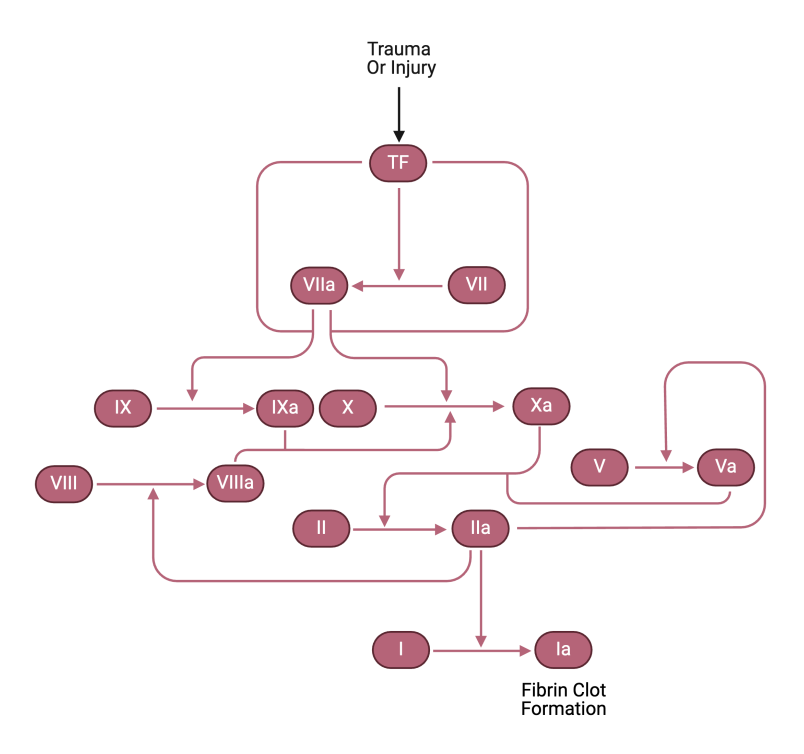


Figure 2: Simplified's chematic of the extrinsic p athway of coagulation. The p athway is initiated with trauma or injury and results in fibrin clot formation. Note that TF represents tissue factor and Ha represents thrombin.

There are two main inhibitors of thrombin generation in the extrinsic pathway: tissue factor pathway inhibitor (TFPI) and antithrombin (AT). TFPI mainly inhibits factor Xa and can bind Xa alone or while in a complex with TF:VIIa [7]. TFPI controls the initiation phase of coagulation, while the other prominent inhibitor, antithrombin, controls the final stages of thrombin generation. Antithrombin inhibits prothrombin directly and indirectly by irreversibly binding to and thereby inactivating factors Xa, IXa, IIa, TF:VIIa, and meizothrombin (mIIa) [1]. This irreversible binding occurs in the solution phase. The inhibitory action of antithrombin is more consequential for factors Xa and IIa, whereas inhibition of the other enzymes is minor [20]. Antithrombin plays a critical role in monitoring the cascade and maintaining a proper hemostatic balance.

1.2. Previous Mathematical Models of Coagulation. One of the first comprehensive mathematical models of coagulation, the Hockin-Mann model, models thrombin generation using the reactions mentioned above of the extrinsic pathway [7]. The reaction list is shown in Table 5. The authors explore the pro- and anti- coagulant mechanisms that are involved in maintaining the balance of blood fluidity by altering certain initial conditions. Hockin et al. show a variety of results, including the effects of tissue factor and different inhibitors [7]. Within their coagulation model, several enzymatic reactions are represented using the scheme in (1.3), where enzymes are not tracked in intermediate states, and thus, their concentrations remain unchanged throughout the reaction. This assumption is applied to the catalytic activity of factor Xa on prothrombin, meizothrombin on prothrombinase, TF:VIIa, factor Xa, and thrombin on factor VII, and to thrombin on factors VIII and V. Notably, factor Xa, thrombin, and TF:VIIa each act on multiple substrates; thus, neglecting substrate competition for enzyme binding likely leads to an overestimation of catalytic activity.

Two additional mathematical models, the Lakshmanan model and the Danforth model, extend the Hockin-Mann model [12] [4]. The Danforth model is shown in Table 6, and the Lakshmanan model in Table 7. Both models incorporate all of the Hockin-Mann reactions and add additional reactions. Thus, the one-step reactions from the Hockin-Mann model are also present in both the Lakshmanan and Danforth models. The Danforth model adds two one-step reactions involving the activation of factor V and factor X. The Lakshmanan model adds fourteen new reactions to the Hockin-Mann model, including three one-step reactions of TF:VII activation and eleven two-step reactions involving factors XI and IX, which are of the form (1.1). In this model, factor XI is activated by thrombin and is inhibited by antithrombin and C1-inhibitor. Factor XI also activates factor IX, which in turn activates factor X.

The Hockin-Mann, Danforth, and Lakshmanan models use a biochemical reaction scheme to form the model. Biochemical reactions, both in coagulation and more generally, involve substrates (S), enzymes (E), intermediate substrate-enzyme complexes (C), and products (P). The reactions proceed via rate constants, denoted as the on rate, off rate, and catalytic rate. Two-step reactions follow the reaction scheme in (1.1).

(1.1)
$$S + E \xrightarrow{k_{on}} C \xrightarrow{k_{cat}} P + E$$

Using the law of mass action, the above biochemical reaction can be written as a system of ordinary differential equations (ODEs), which is shown in (1.2). Variables S, E, C, and P in (1.1) and (1.2) are represented in units of concentration.

(1.2)
$$\frac{dS}{dt} = -k_{on}[S][E] + k_{off}[C]$$

$$\frac{dE}{dt} = -k_{on}[S][E] - k_{off}[C] + k_{cat}[C]$$

$$\frac{dC}{dt} = k_{on}[S][E] - k_{off}[C] - k_{cat}[C]$$

$$\frac{dP}{dt} = k_{cat}[C]$$

The three models follow this reaction scheme for most reactions but choose to use a one-step reaction scheme for a few of the coagulation reactions. These one-step reactions follow the

reaction scheme in (1.3).

$$(1.3) S + E \xrightarrow{k_{cat}} P + E$$

This reaction scheme would result in the following system of differential equations in (1.4)

(1.4)
$$\frac{dS}{dt} = -k_{cat}[S][E]$$

$$\frac{dP}{dt} = k_{cat}[S][E]$$

It is evident that many of the biochemical interactions are being lost. Enzymes are involved in the reaction, but there is no net change in enzyme concentration over time, as described by the ODE system in (1.5). In addition, the binding process between the substrate and the enzyme is disregarded, and no intermediate complex is formed.

(1.5)
$$\frac{dE}{dt} = -k_{cat}[S][E] + k_{cat}[S][E] = 0$$

The remainder of this paper will investigate the problems identified by the Hockin-Mann, Danforth, and Lakshmanan models, as all three of these models use a combination of reactions in the forms (1.1) and (1.3). In each of these three models, we modify the one-step reactions to become two-step reactions. We find that these modifications lead to a reduction of available enzyme and delay the onset of thrombin generation.

2. Methods. Initially, we implement the Hockin-Mann, Danforth, and Lakshmanan models into a baseline "literature model", replicating the reactions, initial conditions, and kinetic rates as in the respective papers. The initial conditions of the literature models are shown in Table 4, and the full reaction sets are shown in Tables 5-7. The reaction schemes are converted to a stoichiometric matrix and written as a system of ODEs using the law of mass action.

We next consider one-step reactions, which omit the intermediate complex as shown in (1.3). When the intermediate step is not included, the substrates and enzymes do not form a complex and thus remain in their "free form" for a longer period. In this case, the enzyme is always available for consumption, giving the appearance of unlimited catalytic capacity. This assumption is not accurate for the blood coagulation pathway. As a result, we modify all reactions of the form (1.3) to reactions of the form (1.1), changing the ODEs from (1.4) to (1.2). In two-step reactions, the enzyme binds the substrate to form an intermediate complex and then releases after product formation. During this time, the enzyme is sequestered and unavailable for other substrates, creating competition that more accurately reflects blood coagulation. These modified two-step reactions introduce an increase in complexity by incorporating new rate constants into the system. We obtain the kinetic rates from these two-step reactions from various sources in the literature. When the literature does not explicitly state k_{on} and k_{off} , but reports their ratio in the form of a dissociation constant, $K_D = \frac{k_{off}}{k_{on}}$, we calculate k_{on} using $k_{on} = \frac{k_{off}}{K_D}$ while assuming k_{off} falls between 0.1 and 10 s^{-1} [11].

We maintain the feasible assumptions made in the Hockin-Mann, Danforth, and Laksh-

We maintain the feasible assumptions made in the Hockin-Mann, Danforth, and Lakshmanan models. All three literature models assume a static fluid environment, as in experimental environments, as opposed to a dynamic fluid environment found in vivo. These models

also assume that some of the unknown rates can be derived from analogous reactions. For example, in the Hockin-Mann model, the rate of factor Xa binding TF:VIIa was unknown at the time the article was written, but the authors assumed that this reaction is analogous to factor X binding TF:VIIa. This assumption is feasible and is often used in other mathematical models of coagulation. We also use this assumption to justify the rates of two two-step reactions that do not have any literature references (see footnotes on pages 6-7).

The one-step Hockin-Mann reactions, the respective two-step reactions, and the kinetic rates are shown in Table 1. The one-step and two-step reactions for the Danforth model and the Lakshmanan model are shown in Table 2 and Table 3, respectively.

One-Step Reaction Two-Step Reaction $k_{off} (s^{-1})$ $(M^{-1}s^{-1})$ $(M^{-1}s^{-1}$ (s^{-1}) 5 [2] $Xa + VII \rightarrow Xa + VIIa$ 1.3e7 $Xa + VII \Leftrightarrow Xa:VII \rightarrow Xa + VIIa$ 5e6 [2] 1 [2] $IIa + VII \rightarrow IIa + VIIa$ $IIa + VII \Leftrightarrow IIa:VII \to IIa + VIIa$ 6.1e-2[2]2.3e43.92e5 [2] 1 [2] $Xa + II \rightarrow Xa + IIa$ 7.5e3 $Xa + II \Leftrightarrow Xa:II \rightarrow Xa + IIa$ 1.03e8 [16] 1 [16] 6.2e-3 [10] $IIa + VIII \rightarrow IIa + VIIIa$ 0.9[6]Ha + VIII ⇔ Ha:VIII → Ha + 1 [14] 2e7VIIIa 2.64e7 [14] $IIa \, + \, V \rightarrow IIa \, + \, Va$ 2e7 $IIa + V \Leftrightarrow IIa:V \to IIa + Va$ 1.73e7 [17] 1 [17] 0.23[17] $TF:VIIa + VII \rightarrow TF:VIIa + VIIa$ $TF:VIIa + VII \Leftrightarrow TF:VIIa:VII \to TF:VIIa + VIIa$ $1e7^*$ 3* 4.4e51* $mIIa\,+\,Xa{:}Va\,\rightarrow\,IIa\,+\,Xa{:}Va$ 1.5e7mII
a + Xa:Va \Leftrightarrow mIIa:Xa:Va \to IIa + Xa:Va 1e8 [1] 66 [1] 15 [10]

Table 1: Hockin-Mann One-Step Reactions and Modified Two-Step Versions.

One-step reactions in the Hockin-Mann model and their second-order rates are shown in the left half of the table. The left half reaction rates are found in the Hockin et al. paper [7]. Then, each of these are modified to include an intermediate complex, as shown in the right half of the table. Literature values for the two-step reactions come from various sources and are shown on the right.

	Table 2: Danforth	One-Step	Reactions	and Modified	Two-Step	Versions.
--	-------------------	----------	-----------	--------------	----------	-----------

One-Step Reaction	k_{cat}	Two-Step Reaction	k_{on}	k_{off}	k_{cat}
	$(M^{-1}s^{-1})$		$(M^{-1}s^{-1})$	(s^{-1})	(s^{-1})
$Xa + VII \rightarrow Xa + VIIa$	1.3e7	$Xa + VII \Leftrightarrow Xa:VII \rightarrow Xa + VIIa$	5e6 [2]	1 [2]	5 [2]
$IIa + VII \rightarrow IIa + VIIa$	2.3e4	$IIa + VII \Leftrightarrow IIa:VII \rightarrow IIa + VIIa$	3.92e5 [2]	1 [2]	6.1e-2 [2]
$Xa + II \rightarrow Xa + IIa$	7.5e3	$Xa + II \Leftrightarrow Xa:II \rightarrow Xa + IIa$	1.03e8 [16]	1 [16]	6.2e-3 [10]
$IIa + VIII \rightarrow IIa + VIIIa$	2e7	$IIa + VIII \Leftrightarrow IIa:VIII \rightarrow IIa + VIIIa$	2.64e7 [14]	1 [14]	0.9 [6]
$IIa + V \rightarrow IIa + Va$	2e7	$IIa + V \Leftrightarrow IIa:V \rightarrow IIa + Va$	1.73e7 [17]	1 [17]	0.23 [17]
TF:VIIa + VII → TF:VIIa + VIIa	4.4e5	$TF:VIIa + VII \Leftrightarrow TF:VIIa:VII \rightarrow TF:VIIa + VIIa$	1e7*	1*	3*
$mIIa + Xa:Va \rightarrow IIa + Xa:Va$	1.5e7	$mIIa + Xa:Va \Leftrightarrow mIIa:Xa:Va \rightarrow IIa + Xa:Va$	1e8 [1]	66 [1]	15 [10]
$IXa + X \rightarrow IXa + Xa$	5.7e3	$IXa + X \Leftrightarrow IXa:X \rightarrow IXa + Xa$	1e8 [19]	14 [19]	8.7e-4 [19]
$mIIa + V \rightarrow mIIa + Va$	3e6	$mIIa + V \Leftrightarrow mIIa:V \rightarrow mIIa + Va$	1e8 [1]	6.94 [1]	1.035 [1]

Similarly to Table 1, one-step Danforth reactions and their rates found in the Danforth et al. paper are shown in the left half [4]. Two-step reactions and their literature sources are shown on the right.

^{*}These reaction rates are chosen by the authors as no literature rates are available. We choose the k_{off} rate to be 1 to be consistent with the other k_{off} rates. We choose the k_{on} to be 1e7 as many tissue factor rates have a k_D around 1e-7 M [2] [11]. We choose a moderate k_{cat} that is close to the value for tissue factor activation by Xa [2]. Varying each of these rates by three orders of magnitude in either direction did not change the thrombin curves (data not shown), so we conclude that these rates are not sensitive to the global model.

One-Step Reaction	k_{cat}	Two-Step Reaction	k_{on}	k_{off}	k_{cat}
one step Headersh	$(M^{-1}s^{-1})$	Two step redection	$(M^{-1}s^{-1})$	(s^{-1})	(s^{-1})
$Xa + VII \rightarrow Xa + VIIa$	2.5e9	$Xa + VII \Leftrightarrow Xa:VII \rightarrow Xa + VIIa$	5e6 [2]	1 [2]	5 [2]
$IIa + VII \rightarrow IIa + VIIa$	2.3e4	$IIa + VII \Leftrightarrow IIa:VII \rightarrow IIa + VIIa$	3.92e5 [2]	1 [2]	6.1e-2 [2]
$Xa + II \rightarrow Xa + IIa$	9.2e3	$Xa + II \Leftrightarrow Xa:II \rightarrow Xa + IIa$	1.03e8 [16]	1 [16]	6.2e-3 [10]
$IIa + VIII \rightarrow IIa + VIIIa$	2.5e7	$IIa + VIII \Leftrightarrow IIa:VIII \rightarrow IIa + VIIIa$	2.64e7 [14]	1 [14]	0.9 [6]
$IIa + V \rightarrow IIa + Va$	2.3e7	$IIa + V \Leftrightarrow IIa:V \rightarrow IIa + Va$	1.73e7 [17]	1 [17]	0.23 [17]
$TF:VIIa + VII \rightarrow TF:VIIa + VIIa$	4.4e5	$TF:VIIa + VII \Leftrightarrow TF:VIIa:VII \rightarrow TF:VIIa + VIIa$	1e7*	1*	3*
$mIIa + Xa:Va \rightarrow IIa + Xa:Va$	2.3e7	$mIIa + Xa:Va \Leftrightarrow mIIa:Xa:Va \rightarrow IIa + Xa:Va$	1e8 [1]	66 [1]	15 [10]
TF:VIIa + TF:VII \rightarrow 2 TF:VIIa	4.4e5	$TF:VIIa + TF:VII \Leftrightarrow TF:VIIa:TF:VII \rightarrow 2 TF:VIIa$	1e7*	1*	3*
$Xa + TF:VII \rightarrow Xa + TF:VIIa$	2.5e9	$Xa + TF:VII \Leftrightarrow Xa:TF:VII \rightarrow Xa + TF:VIIa$	5e7 [2]	44.8 [2]	15.2 [2]
$IIa + TF:VII \rightarrow IIa + TF:VIIa$	2.3e4	$IIa + TF:VII \Leftrightarrow IIa:TF:VII \rightarrow IIa + TF:VIIa$	3.92e5 [2]	1 [2]	6.1e-2 [2]

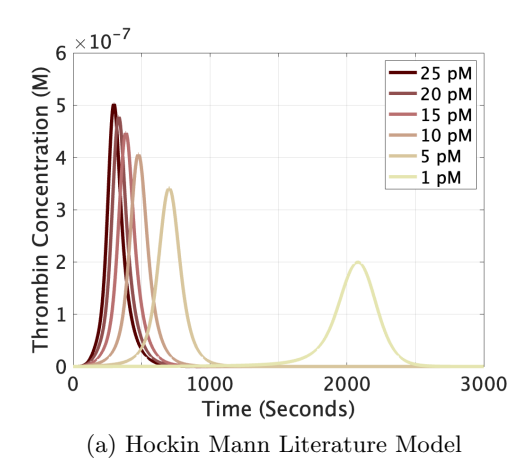
Table 3: Lakshmanan One-Step Reactions and Modified Two-Step Versions.

Similarly to Table 1, one-step Lakshmanan reactions and their rates found in the Lakshmanan et al. paper are shown in the left half [12]. Two-step reactions and their literature sources are shown on the right.

The literature and modified versions of the Hockin-Mann, Danforth, and Lakshmanan models are implemented in MATLAB and solved using the MATLAB stiff differential equation solver ode15s [9]. Since the species are measured in concentration, the system of ODEs models the change in concentration over time. We analyze the effect of intermediate complex formation by comparing simulated thrombin dynamics with the two versions of each model. We also analyze the effect of the inhibitors TFPI and antithrombin.

- 3. Results And Discussion. Simulations for each model are performed in MATLAB. Figures 3-8 show the concentration of total generated thrombin (mIIa+IIa) as a function of time. The plots can be analyzed by examining a variety of thrombin metrics: peak concentration, time to peak concentration, and lag time. The peak concentration is the highest concentration of thrombin over the time course, and the time to peak refers to the time it takes to reach this peak height. Lag time refers to the time period between the initiation of the coagulation cascade and the generation of 1·10⁻⁹ M of thrombin. A prolonged lag time would refer to a delay in the onset of thrombin production, while a short lag time would refer to a faster initiation, typically associated with a more efficient and effective hemostatic response.
- **3.1.** Hockin-Mann Model. Figure 3 shows the graph of total thrombin produced in the extrinsic pathway of coagulation with different concentrations of tissue factor in picomolar (pM) to initiate the cascade. The original Hockin-Mann study defines 25 pM of tissue factor as the base case and varies concentrations from 1 pM to 25 pM to examine coagulation responses. In these models, thrombin is solely initiated by tissue factor, so a concentration of 0 pM tissue factor would result in a zero thrombin curve. Figure 3a reproduces Hockin et al.'s plot of thrombin generation versus time. For the 25 pM base case in this model, we see a lag time of approximately 125 seconds, a peak time of 300 seconds, and a peak thrombin

^{*}Similarly to the reactions in the Hockin-Mann and Danforth models, these reaction rates are chosen for both TF:VIIa activation of VII and TF:VIIa autoactivation. Varying each of these rates by three orders of magnitude in either direction did not change the thrombin curves (data not shown), so we conclude that these rates are not sensitive to the global model.



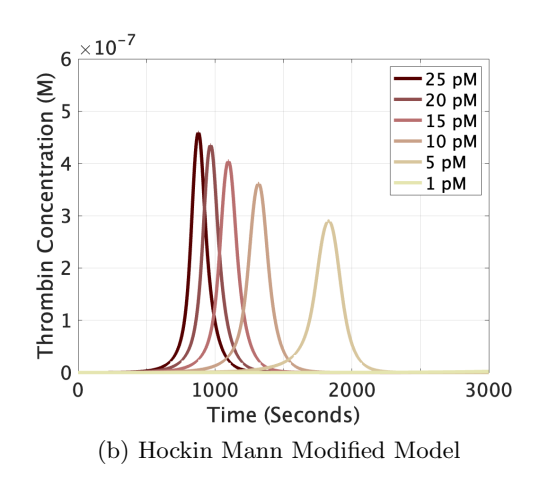
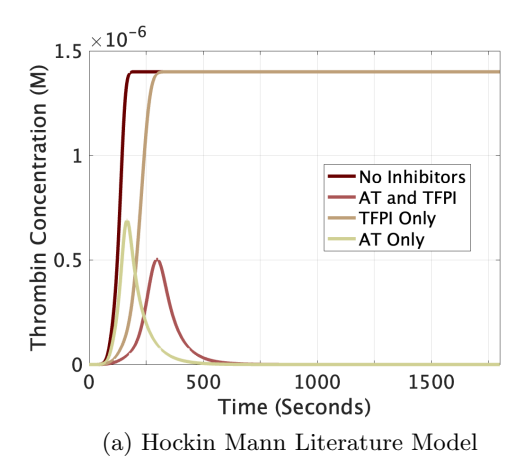


Figure 3: Total thrombin (IIa + mIIa) as a function of time is represented for varying initial tissue factor concentrations.

concentration of around $5 \cdot 10^{-7}$ M. These values are shown more clearly in Figures 9a-9c. As the concentration of tissue factors decreases, the lag time and the time to the peak concentration increase since thrombin takes longer to generate. With less tissue factor, we also see a lower peak concentration of thrombin. Note that 1 pM results in a nonzero thrombin curve that exceeds the time scale of the plot.

Figure 3b shows total thrombin dynamics using modified equations and kinetic r ates. As shown in the plot and Figures 9a-9c, the base case produces a lag time of approximately 650 seconds, a peak time at 880 seconds, and a peak concentration of around $4.5 \cdot 10^{-7}$ M. The plot follows the same trend as the literature Hockin-Mann model: decreased levels of tissue factor result in a longer thrombin generation period and lower peak thrombin. In comparison with Figure 3a, the model is qualitatively similar, producing bell-shaped curves that follow the same trend with a similar time period in between lag time and peak time: 175 seconds in Figure 3a and 230 seconds in Figure 3b for 25 pM tissue factor. Each of the other tissue factor concentrations has similar times between the lag time and peak time, except for the 1 pM curve.

There are some distinguishable differences between Figures 3a and 3b. The most notable is that the modified Hockin-Mann model requires more time to initiate and reach peak thrombin production. The modified model requires approximately three times the time as the literature model to reach its peak, indicating that there is a difference in time scale between the reaction schemes of the literature and modified models. The modified model's curves are also more spread out; the difference in peak time between 25 pM and 20 pM is 80 seconds for Figure 3b, while only 35 seconds for Figure 3a. This trend is observed between each peak for the two plots; for example, the 25 pM and 5 pM curves in Figure 3a are relatively closer than the 25 pM and 5 pM curves in Figure 3b. The thrombin delay in Figure 3b is likely due to species from the modified model (VII, VIII, V, and thrombin) first forming an intermediate complex before activation.



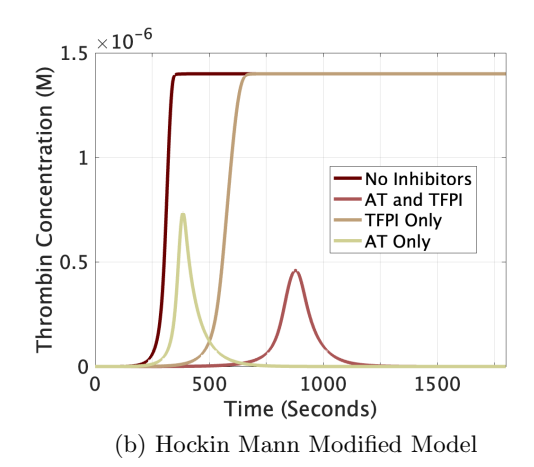


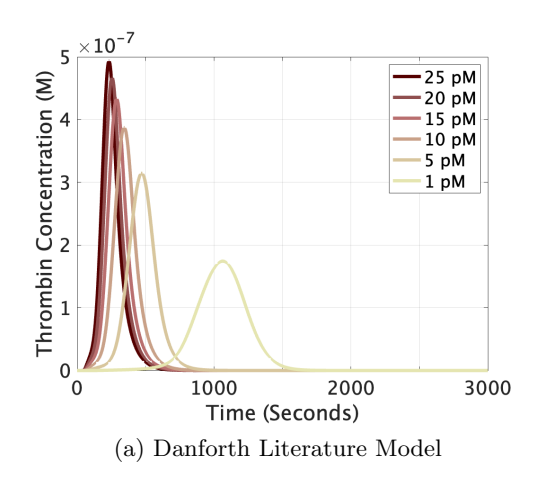
Figure 4: Active thrombin as a function of time for a reaction initiated by 25 pM tissue factor with inhibitors antithrombin and TFPI.

Figure 4 illustrates the effect that antithrombin and TFPI have on the active thrombin dynamics. In this figure, the simulations including antithrombin yield bell-shaped c urves. This strengthens the idea that antithrombin acts as an inhibitor in the final stages of thrombin generation. Without antithrombin, thrombin reaches and maintains a high peak concentration, and the absence of regulatory control results in a sustained non-zero steady state. The simulated results show that TFPI is more involved in the initiation phase since we see a decrease in peak thrombin, but the final concentration is still regulated.

Qualitatively, Figures 4a and 4b are similar, and the peak thrombin concentrations do not deviate much between Figures 4a and 4b. The main difference between these two figures is the timing. Similarly to Figure 3b, Figure 4b exhibits a longer lag time, time to peak, and time in between each curve than Figure 4a. The likely explanation is that species in two-step reactions require additional time to be activated, prolonging thrombin generation. However, since the inhibition reaction equations remain unchanged between the two models, both graphs exhibit similar qualitative behavior. The key difference is t hat modifications made to reactions without inhibitors have a greater impact on the timing of the TFPI curves than on the timing of the antithrombin curves. The timing of the curves with TFPI (the AT+TFPI and TFPI-only curves) is drastically prolonged in Figure 4b in comparison to the other curves.

In comparing the literature and modified Hockin-Mann models, the results are qualitatively similar. Each curve depicted in Figures 3 and 4 closely mirrors the corresponding curve in the other, displaying similar curves and peak values. Notably, the introduction of an intermediate step in the modified two-step scheme extends the time scale across all reproduced figures. This time scale delay is likely a consequence of an additional activation step required for the species in the two-step reaction.

3.2. Danforth Model. For the Danforth model, we simulate thrombin generation curves over time as in the Hockin-Mann model. Figure 5a shows the literature reproduction of total thrombin generation with the same tissue factor concentrations in the Hockin-Mann model. Figure 5b is a simulation of the modified model, which includes intermediate complexes and their respective literature rates. These plots differ by their peak thrombin concentration, time to peak, and lag time. For each tissue factor concentration, the peak thrombin in the literature Danforth model is greater than the modified model. Additionally, the modified model takes more than twice as long to reach a peak thrombin generation for each tissue factor concentration. Similar to the Hockin-Mann models, differences between the literature and modified Danforth models can be attributed to intermediate complexes that impact timing by reducing the availability of free species. However, the change in peak thrombin concentration must be due to the reactions unique to the Danforth model, as we see a peak height difference between Figures 5a and 5b, but do not see the peak height noticeably change between Figures 3a and 3b. Peak thrombin is sensitive to the reactions from Table 2, so altering these two new reactions, shown in the bottom two rows of Table 2, affects the system.



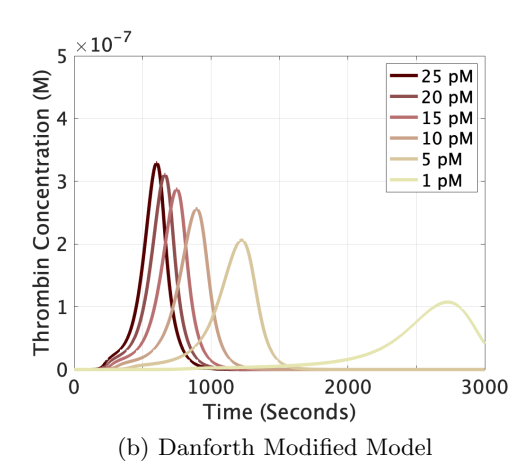
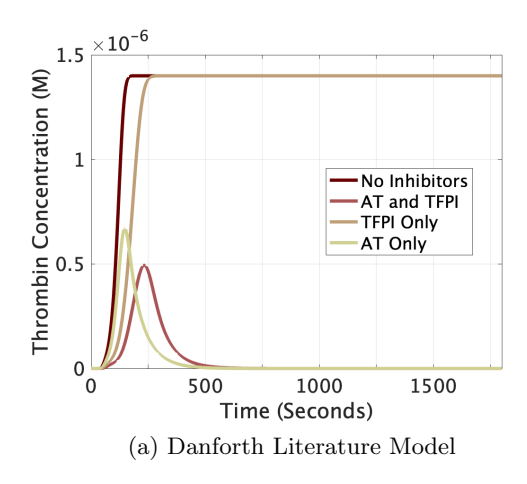


Figure 5: Total thrombin (IIa + mIIa) as a function of time is represented for varying initiating tissue factor concentrations.

Figure 5b displays a slower onset of thrombin generation than Figure 5a. For example, in the 25 pM tissue factor curve, the literature model displays a steep initial rise, indicating rapid thrombin generation following the lag phase. In contrast, in the modified model, thrombin generation increases more gradually up to around 400 seconds, after which the rate of increase becomes slightly steeper until it reaches its peak. This is likely due to the last reaction in Table 2. The one-step literature reaction involves no competition for meizothrombin since there is no change in the meizothrombin ODE due to this reaction. In the two-step reaction, there is less free meizothrombin since more meizothrombin is now found in the complex mHa:V. This leads to a slower onset of total thrombin generation.

Simulating various combinations of inhibitors AT and TFPI in the literature and the modified Danforth model led to similar results as the Hockin-Mann model. For example, the



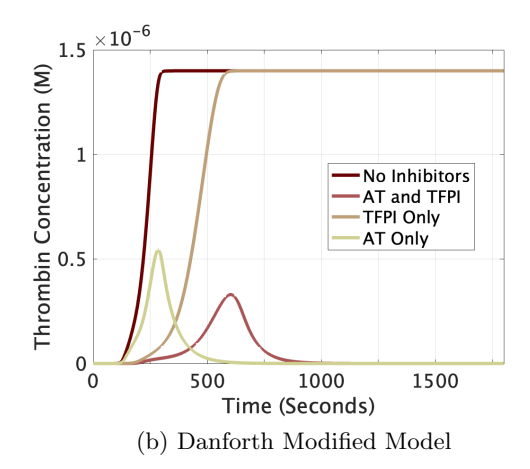


Figure 6: Active thrombin as a function of time for a reaction initiated by 25 pM tissue factor with inhibitors antithrombin and TFPI.

timing of the curves with TFPI (the AT+TFPI and TFPI-only curves) are more prolonged in Figure 6b in comparison to curves without TFPI (no inhibitors and AT-only). Additionally, the shape of the curve with both inhibitors has more sustained thrombin generation, and the time between the lag and peak time is greater in Figure 6b for this curve. Overall, Figure 6 is qualitatively similar to Figure 4, but the timing in the modified model is delayed.

3.3. Lakshmanan Model. The mathematical model by Lakshmanan et al. is also based on the Hockin-Mann model. The Lakshmanan model contains ten reactions that use a one-step reaction scheme without intermediate complexes. Lakshmanan et al. then estimates each kinetic rate using the Sequential Least Squares Programming algorithm in SciPy against experimental data they collected; thus, the kinetic rates for the Lakshmanan model are different from the Hockin-Mann and Danforth models. We simulate both the literature and the modified model with Lakshmanan et al.'s estimated rates and the same tissue factor concentrations that appear in Figures 3 and 5. The modified model includes first-order reaction rates, and these rates are derived from various literature sources.

Unlike the aforementioned Hockin-Mann and Danforth models, the literature and modified Lakshmanan models do not look much different at first gl ance. Compared to the literature model in Figure 7a, the Lakshmanan modified model in Figure 7b has a later lag and peak time for each thrombin curve. These differences are displayed more clearly in Figure 9. Although the differences in lag time and peak time between the literature and modified models are not as drastic as the Hockin-Mann and Danforth models, there is still a 1-2 minute delay in lag and peak time in the modified model.

We then examine the effects of a dding AT and TFPI individually and in combination. The literature and modified models show few differences, with each modified curve closely resembling its respective literature curve. Similarly to Figure 7, it is difficult to notice the differences, but the lag time and peak time are delayed by 1-2 minutes. However, the Lak-

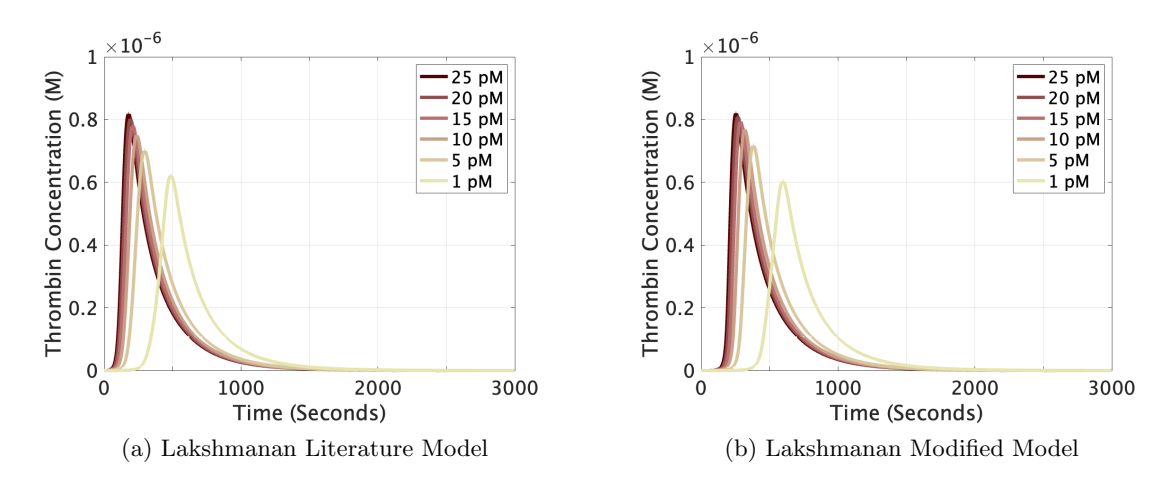


Figure 7: Total thrombin (IIa + mIIa) as a function of time is represented for varying initiating tissue factor concentrations.

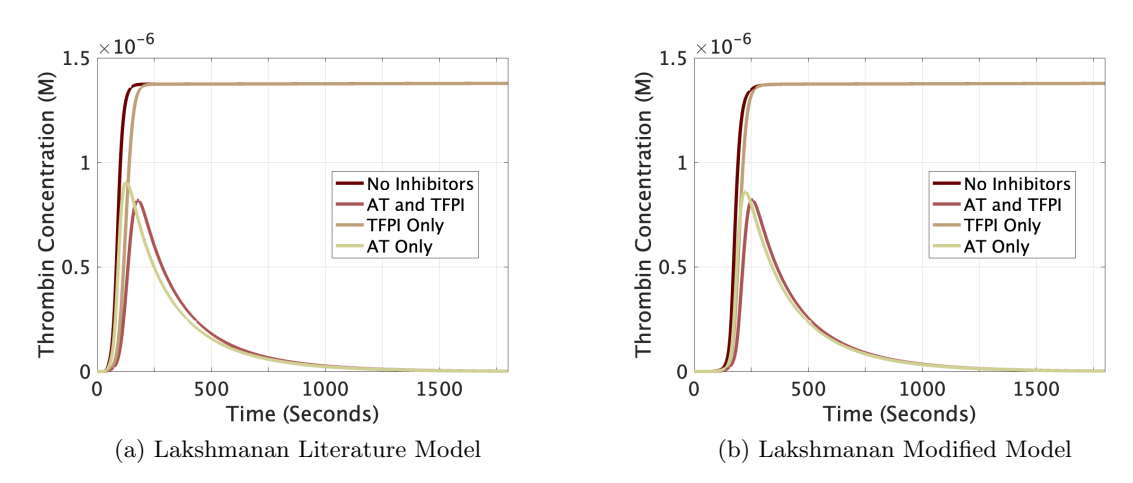


Figure 8: Active thrombin as a function of time for a reaction initiated by 25 pM tissue factor with inhibitors antithrombin and TFPI.

shmanan inhibitor graphs differ from the Hockin-Mann and Danforth graphs, as TFPI has minimal effect on the system. The differences between the no-inhibitor curve and the TFPI-only curve are slight, as are the differences between the AT-only and AT+TFPI curves in Figures 8a and 8b.

Although the literature and modified graphs appear similar, the underlying biochemical kinetics and reaction rates differ s ignificantly. As previously described, the original Lakshmanan study uses the reaction scheme shown in (1.4) for one-step reactions. In this scheme, more free enzymes are available, and no species compete for these enzymes because the enzyme concentrations are independent of the reactions they catalyze. In contrast, the modified

model includes additional intermediate species, resulting in more complexes that sequester enzymes. This added competition is not taken into account in the original Lakshmanan study. However, the literature Lakshmanan model fits the reaction rates using experimental data. This corrects for the changes made by introducing one-step equations. Although the model ends up matching experiments—due to estimated rates—this approach may obscure important differences introduced by the modified two-step reaction scheme, oversimplifying the true biochemical dynamics of the system.

3.4. Thrombin Metrics for Each Model. To further assess the impact of changing one-step reactions to two-step reactions using literature values, we plotted key thrombin metrics for both the literature and modified versions of each model. The peak height, peak time, and lag time thrombin metrics were calculated for the range of tissue factor concentrations shown in the previous graphs. By comparing these values between the literature and modified models, we can gain insight into how altering reactions affect thrombin dynamics and quantify what is seen in the previous graphs with various tissue factor concentrations.

Figure 9 shows that for the Hockin-Mann model, modifications c hange the t iming the most. Lower tissue factor concentrations are the most affected, with reduced tissue factor leading to the greatest changes in both lag time and peak time. The Danforth model is also impacted by the modifications, with decreased peak height and delays in all timing metrics. A notable distinction between the Hockin-Mann and Danforth models is that the Hockin-Mann model exhibits a significantly longer lag time, whereas the Danforth model accelerates thrombin generation in both the literature and modified versions, though at a lower peak height than the Hockin-Mann models. The Lakshmanan model, by contrast, produces a much higher peak height and achieves even faster timing. However, differences in timing persist between the literature and modified versions of the Lakshmanan model, although to a lesser extent.

4. Conclusions. Using mathematical modeling, we have shown how reactions with and without an intermediate complex affect systems of biochemical r eactions. The modifications introduced in these models—specifically, the inclusion of intermediate complexes and the transition from one-step to two-step reactions—aim to improve the mechanistic consistency of the system and more accurately reflect the biochemical nature of coagulation processes. The omission of an intermediate complex underscores complex interactions between enzymes, substrates, and cofactors involved in coagulation. Modifying these reactions to create modified versions of the Hockin-Mann, Danforth, and Lakshmanan models plays a crucial role in refining simulations, optimizing experimental designs, and ultimately advancing our understanding of blood coagulation.

While these modifications make the models more accurate from a biochemical perspective, they also introduce new challenges. The addition of intermediate complexes—while necessary for biological accuracy—slows down the overall model kinetics of thrombin generation. The introduction of these intermediates creates additional steps and competition for enzymes within the simulation, leading to a delay in lag time and peak time that deviate significantly from the actual rapid dynamics observed in vivo.

However, we cannot simply revert to the one-step reactions or ignore these intermediates to regain the speed of thrombin generation because doing so would undermine the biological

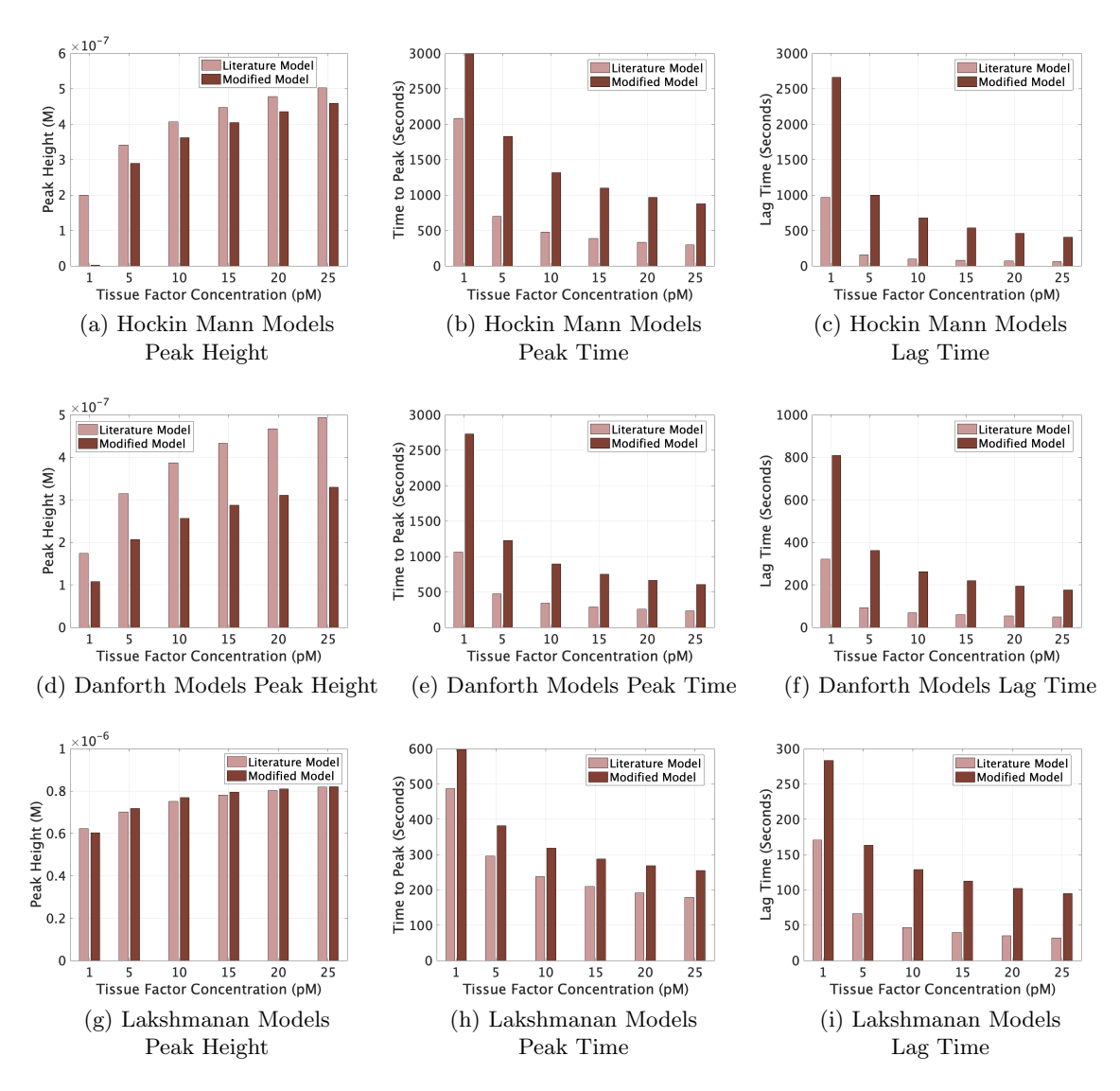


Figure 9: Thrombin metrics for literature and modified versions of each mathematical model.

relevance of the model. It is also insufficient to solely estimate every rate against experimental data, as the original Lakshmanan study does, since Lakshmanan et al. still include one-step reactions. The timing delays in the Hockin-Mann, Danforth, and Lakshmanan modified models suggest that these models might still be missing some key features. It is also possible that some reaction rates in the original literature studies may be inaccurate, or the models are still missing reactions or feedback loops that have not been included in the models. For example, some rate constants the models are using may be slower than what is true.

The results of this study underscore the importance of refining computational models to include intermediate steps that were previously overlooked. Although the inclusion of inter-

MODIFYING ONE-STEP COAGULATION REACTIONS

mediate complexes improves the biological and kinetic accuracy of the models, it introduces delays that may not match the true timing of thrombin generation. Among the Hockin et al. and Lakshmanan et al. papers are a few plots of experimental thrombin generation [7] [12]. The timing delay in the modified models suggests that further work is needed in refining these models, possibly through further investigation of kinetic rates or by incorporating additional biochemical reactions that are currently unaccounted for.

There are other mathematical models of coagulation that use only intermediate complexes in reaction schemes. Some models use a static environment, like the models explored in our study, while others consider flow. Various models rely on different sets of reactions and kinetic rates, which makes it challenging to interpret these models in the field [18]. Thus, future work in the field needs to refine reaction network components and rate constants.

Appendix A. Initial Conditions and Full Reaction List for Each Model.

Table 4: Mathematical Model Nonzero Initial Conditions.

Coagulation Factor	Initial Condition (nM)
Tissue Factor (TF)	Varying
Prothrombin (II)	1400 [7]
Factor V	20 [7]
Factor VII	10 [7]
Factor VIIa	0.1 [7]
Factor VIII	0.7 [7]
Factor IX	90 [7]
Factor X	160 [7]
Factor XI	30 [12]
TFPI	2.5 [7]
Antithrombin (AT)	3400 [7]
C1-Inhibitor (C1INH)	2500 [12]

Initial conditions equal normal blood plasma concentrations. The initial conditions are the same across all models as Lakshmanan and Danforth models draw from the Hockin-Mann model, but only the Lakshmanan model has factor XI and C1-inhibitor present. The Lakshmanan et al. article uses these initial conditions but multiplies each by 0.4. We choose not to multiply initial conditions by 0.4 for consistency across each model.

Table 5: Hockin-Mann Full Reaction List.

Reaction	k_{on}	k_{off}	k_{cat}
	$(M^{-1}s^{-1})$	(s^{-1})	(s^{-1})
$TF + VII \Leftrightarrow TF:VII$	3.2e6	3.1e-3	
$TF + VIIa \Leftrightarrow TF:VIIa$	2.3e7	3.1e-3	
$TF:VIIa + VII \rightarrow TF:VIIa + VIIa$			4.4e5*
$Xa + VII \rightarrow Xa + VIIa$			1.3e7*
$IIa + VII \rightarrow IIa + VIIa$			2.3e4*
$TF:VIIa + X \Leftrightarrow TF:VIIa:X \rightarrow TF:VIIa:Xa$	2.5e7	1.05	6
TF:VIIa + Xa ⇔ TF:VIIa:Xa	2.2e7	19	
$TF:VIIa + IX \Leftrightarrow TF:VIIa:IX \rightarrow TF:VIIa + IXa$	1e7	2.4	1.8
$Xa + II \rightarrow Xa + IIa$			7.5e3*
$IIa + VIII \rightarrow IIa + VIIIa$			2e7*
VIIIa + IXa ⇔ IXa:VIIIa	1e7	5e-3	
$ IXa:VIIIa + X \Leftrightarrow IXa:VIIa:X \rightarrow IXa:VIIIa + Xa$	1e8	1e-3	8.2
$VIIIa \Leftrightarrow VIIIa_1 + VIIIa_2$	6e-3	2.2e4	
$IX:VIIIa:X \rightarrow VIIIa_1 + VIIIa_2 + X + IXa$	1e-3		
$ IXa:VIIIa \rightarrow VIIIa_1 + VIIIa_2 + IXa $	1e-3		
$IIa + V \rightarrow IIa + Va$			2e7*
Xa + Va ⇔ Xa:Va	4e8	0.2	
$Xa:Va + II \Leftrightarrow Xa:Va:II \rightarrow Xa:Va + mIIa$	1e8	103	63.5
$mHa + Xa:Va \rightarrow Ha + Xa:Va$			1.5e7*
$Xa + TFPI \Leftrightarrow Xa:TFPI$	9e5	3.6e-4	
TF:VIIa:Xa + TFPI ⇔ TF:VIIa:Xa:TFPI	3.2e8	1.1e-4	
$TF:VIIa + Xa:TFPI \rightarrow TF:VIIa:Xa:TFPI$	5e7		
$Xa + ATIII \rightarrow Xa:ATIII$	1.5e3		
$mIIa + ATIII \rightarrow mIIa:ATIII$	7.1e3		
$IXa + ATIII \rightarrow IXa:ATIII$	4.9e2		
$IIa + ATIII \rightarrow IIa:ATIII$	7.1e3		
$ ext{TF:VIIa} + ext{ATIII} o ext{TF:VIIa:ATIII}$	2.3e2		

The full reaction list and rates as found in Hockin et al. [7]. Note that some table entries are blank, as not all reactions involve both binding and activation.

MODIFYING ONE-STEP COAGULATION REACTIONS

Table 6: Danforth Full Reaction List.

Reaction	k_{on}	k_{off}	k_{cat}
	$(M^{-1}s^{-1})$	(s^{-1})	(s^{-1})
$TF + VII \Leftrightarrow TF:VII$	3.2e6	3.1e-3	
$TF + VIIa \Leftrightarrow TF:VIIa$	2.3e7	3.1e-3	
$ ext{TF:VIIa} + ext{VII} o ext{TF:VIIa} + ext{VIIa}$			4.4e5*
$Xa + VII \rightarrow Xa + VIIa$			1.3e7*
$IIa + VII \rightarrow IIa + VIIa$			2.3e4*
$TF:VIIa + X \Leftrightarrow TF:VIIa:X \rightarrow TF:VIIa:Xa$	2.5e7	1.05	6
$TF:VIIa + Xa \Leftrightarrow TF:VIIa:Xa$	2.2e7	19	
$TF:VIIa + IX \Leftrightarrow TF:VIIa:IX \rightarrow TF:VIIa + IXa$	1e7	2.4	1.8
$Xa + II \rightarrow Xa + IIa$			7.5e3*
$IIa + VIII \rightarrow IIa + VIIIa$			2e7*
VIIIa + IXa ⇔ IXa:VIIIa	1e7	5e-3	
$IXa:VIIIa + X \Leftrightarrow IXa:VIIa:X \rightarrow IXa:VIIIa + Xa$	1e8	1e-3	8.2
$VIIIa \Leftrightarrow VIIIa_1 + VIIIa_2$	6e-3	2.2e4	
$IX:VIIIa:X \rightarrow VIIIa_1 + VIIIa_2 + X + IXa$	1e-3		
$IXa:VIIIa \rightarrow VIIIa_1 + VIIIa_2 + IXa$	1e-3		
$IIa + V \rightarrow IIa + Va$			2e7*
Xa + Va ⇔ Xa:Va	4e8	0.2	
$Xa:Va + II \Leftrightarrow Xa:Va:II \rightarrow Xa:Va + mIIa$	1e8	103	63.5
$mIIa + Xa:Va \rightarrow IIa + Xa:Va$			2.3e8*
$Xa + TFPI \Leftrightarrow Xa:TFPI$	9e5	3.6e-4	
TF:VIIa:Xa + TFPI ⇔ TF:VIIa:Xa:TFPI	3.2e8	1.1e-4	
$TF:VIIa + Xa:TFPI \rightarrow TF:VIIa:Xa:TFPI$	5e7		
$Xa + ATIII \rightarrow Xa:ATIII$	4.2e3		
$mIIa + ATIII \rightarrow mIIa:ATIII$	7.1e3		
$IXa + ATIII \rightarrow IXa:ATIII$	4.9e2		
$IIa + ATIII \rightarrow IIa:ATIII$	7.1e3		
$ ext{TF:VIIa} + ext{ATIII} o ext{TF:VIIa:ATIII}$	2.3e2		
$IXa + X \rightarrow IXa + Xa$			5.7e3*
$mIIa + V \rightarrow mIIa + Va$			3e6 [⋆]

The full reaction list and rates as found in Danforth et al. [4]. Note that some table entries are blank, as not all reactions involve both binding and activation.

Table 7: Lakshmanan Full Reaction List.

Reaction	k_{on}	k_{off}	k_{cat}
Teaction	$(M^{-1}s^{-1})$	(s^{-1})	(s^{-1})
$TF + VII \Leftrightarrow TF:VII$	1.7e5	3e-3	(8)
TF + VIIa ⇔ TF:VIIa	2.2e8	3.1e-5	
$TF:VIIa + VII \rightarrow TF:VIIa + VIIa$	2.200	0.10 0	4.4e5*
$Xa + VII \rightarrow Xa + VIIa$			2.5e9*
IIa + VII → IIa + VIIa			2.3e4*
TF:VIIa + X ⇔ TF:VIIa:Xa	7.5e6	5.2e-1	11
TF:VIIa + Xa ⇔ TF:VIIa:Xa	2.2e7	39	
$TF:VIIa + IX \Leftrightarrow TF:VIIa:IX \rightarrow TF:VIIa + IXa$	2.7e7	4.2e2	10
$Xa + II \rightarrow Xa + IIa$			9.2e3*
$IIa + VIII \rightarrow IIa + VIIIa$			2.5e7*
VIIIa + IXa ⇔ IXa:VIIIa	5e7	2.8e-3	
$IXa:VIIIa + X \Leftrightarrow IXa:VIIa:X \rightarrow IXa:VIIIa + Xa$	1.3e8	1e-3	42
$VIIIa \Leftrightarrow VIIIa_1 + VIIIa_2$	7.5e-3	2.1e4	
$IX:VIIIa:X \rightarrow VIIIa_1 + VIIIa_2 + X + IXa$	1.4e-4		
$IXa:VIIIa \rightarrow VIIIa_1 + VIIIa_2 + IXa$	6.1e-4		
$IIa + V \rightarrow IIa + Va$			2.3e7*
$Xa + Va \Leftrightarrow Xa:Va$	4.9e8	0.3	
$Xa:Va + II \Leftrightarrow Xa:Va:II \rightarrow Xa:Va + mIIa$	2.5e7	78	13
$mIIa + Xa:Va \rightarrow IIa + Xa:Va$			2.3e7*
Xa + TFPI ⇔ Xa:TFPI	2.2e7	3.7e-5	
TF:VIIa:Xa + TFPI ⇔ TF:VIIa:Xa:TFPI	1e7	1e-5	
$ ext{TF:VIIa} + ext{Xa:TFPI} o ext{TF:VIIa:Xa:TFPI}$	4.4e8		
$Xa + ATIII \rightarrow Xa:ATIII$	1.2e3		
$ ext{mIIa} + ext{ATIII} o ext{mIIa:ATIII}$	1e4		
$IXa + ATIII \rightarrow IXa:ATIII$	7e2		
$IIa + ATIII \rightarrow IIa:ATIII$	2.1e3		
$\text{TF:VIIa} + \text{ATIII} \rightarrow \text{TF:VIIa:ATIII}$	3.3e2		
$TF:VIIa + TF:VII \rightarrow TF:VIIa + TF:VIIa$			4.4e5*
$Xa + TF:VII \rightarrow Xa + TF:VIIa$			2.5e9*
$IIa + TF:VII \rightarrow IIa + TF:VIIa$			2.3e4*
$XI + IIa \Leftrightarrow XI:IIa \rightarrow XIa + IIa$	5e7	9.9	1.1e-4
$XIa + IX \Leftrightarrow XIa:IX \rightarrow XIa + IXa$	6.1e5	0.99	0.11
$XIa + ATIII \rightarrow XIa:ATIII$	3.2e2		
$XIa + C1INH \rightarrow XIa:C1INH$	1.8e3		
$IXa + X \Leftrightarrow IXa:X \rightarrow IXa + Xa$	1e8	3.3e2	3e-3

The full reaction list and rates as found in Lakshmanan et al. [12]. Note that some table entries are blank, as not all reactions involve both binding and activation.

^{*}These k_{cat} rates use the second-order rate constant unit of $M^{-1}s^{-1}$ instead of the first-order rate constant unit s^{-1} . These also mark the reactions in Tables 1-3 which were modified.

REFERENCES

- [1] S. D. Bungay, P. A. Gentry, and R. D. Gentry, A mathematical model of lipid-mediated thrombin generation, Math Med Biol., 20 (2003), pp. 105–129, https://doi.org/10.1093/imammb/20.1.105.
- [2] S. Butenas and K. G. Mann, *Kinetics of human factor vii activation*, Biochemistry, 35 (1996), pp. 1904–1910, https://doi.org/10.1021/bi951768c.
- [3] R. Chaudhry, R. B. Killeen, and H. M. Babiker, *Physiology, Coagulation Pathways*, StatPearls Publishing, 2025.
- [4] C. M. DANFORTH, T. ORFEO, K. G. MANN, K. E. BRUMMEL-ZIEDINS, AND S. J. EVERSE, The impact of uncertainty in a blood coagulation model, Math Med Biol., 20 (2009), pp. 323–336, https://doi.org/ 10.1093/imammb/dqp011.
- [5] S. P. GROVER AND N. MACKMAN, Tissue factor: an essential mediator of hemostasis and trigger of thrombosis, Arterioscler Thromb Vasc Biol., 38 (2018), pp. 709–725, https://doi.org/10.1161/ATVBAHA. 117.309846.
- [6] D. C. HILL-EUBANKS AND P. VON LOLLAR, von willebrand factor is a cofactor for thrombin-catalyzed cleavage of the factor viii light chain, Journal of Biological Chemistry, 265 (1990), pp. 17854–17858, https://doi.org/10.1016/S0021-9258(18)38242-5.
- M. F. HOCKIN, K. C. JONES, S. J. EVERSE, AND K. G. MANN, A model for the stoichiometric regulation of blood coagulation, Journal of Biological Chemistry, 277 (2002), pp. 18322–18333, https://doi.org/ 10.1074/jbc.M201173200.
- [8] M. HOFFMAN, D. M. MONROE, J. A. OLIVER, AND H. R. ROBERTS, Factors ixa and xa play distinct roles in tissue factor-dependent initiation of coagulation, Blood, 86 (1995), pp. 1794–1801, https://doi.org/10.1182/blood.v86.5.1794.bloodjournal8651794.
- [9] T. M. Inc., Matlab version: 24.2.0 (r2024b), 2024, https://www.mathworks.com.
- [10] S. Krishnaswamy, W. Church, M. Nesheim, and K. Mann, Activation of human prothrombin by human prothrombinase. influence of factor va on the reaction mechanism, Journal of Biological Chemistry, 7 (1987), pp. 3291–3299, https://doi.org/10.1016/S0021-9258(18)61503-0.
- [11] A. L. Kuharsky and A. L. Fogelson, Surface-mediated control of blood coagulation: The role of binding site densities and platelet deposition, Biophysical Journal, 80 (2001), pp. 1050-1074, https://doi.org/10.1016/S0006-3495(01)76085-7.
- [12] H. H. S. Lakshmanan, A. Estonilo, S. E. Reitsma, A. R. Melrose, J. Subramanian, T. J. Zheng, J. Maddala, E. I. Tucker, D. Gailani, O. J. T. McCarty, P. L. Jurney, and C. Puy, Revised model of the tissue factor pathway of thrombin generation: Role of the feedback activation of fxi, J Thromb Haemost., 20 (2022), pp. 1350–1363, https://doi.org/10.1111/jth.15716.
- [13] K. LEIDERMAN AND A. L. FOGELSON, Grow with the flow: a spatial-temporal model of platelet deposition and blood coagulation under flow, Math Med Biol., 28 (2011), pp. 47–84, https://doi.org/10.1093/ imammb/dqq005.
- [14] P. LOLLAR, G. J. KNUTSON, AND D. N. FASS, "activation of porcine factor viii: C by thrombin and factor xa, Biochemistry, 24 (1985), pp. 8056-8064, https://doi.org/10.1021/bi00348a033.
- [15] S. MCRAE, Mechanisms of Vascular Disease: A Reference Book for Vascular Specialists, University of Adelaide Press, 2011, ch. Physiological Haemostasis.
- [16] R. P. T. MICHAEL E NESHEIM, P. B. TRACEY, D. S. BOSKOVIC, AND K. G. MANN, Mathematical simulation of prothrombinase, Methods in Enzymology, 215 (1992), pp. 316–328, https://doi.org/10. 1016/0076-6879(92)15074-m.
- [17] D. D. Monkovic and P. B. Tracy, Functional characterization of human platelet-released factor v and its activation by factor xa and thrombin, Journal of Biological Chemistry, 265 (1990), pp. 17132–17140, https://doi.org/10.1016/S0021-9258(17)44879-4.
- [18] M. J. OWEN, J. R. WRIGHT, E. G. D. TUDDENHAM, J. R. KING, A. H. GOODALL, AND J. L. DUNSTER, Mathematical models of coagulation-are we there yet?, J Thromb Haemost., 22 (2024), pp. 1689–1703, https://doi.org/10.1016/j.jtha.2024.03.009.
- [19] R. RAWALA-SHEIKH, S. S. AHMAD, B. ASHBY, AND P. N. WALSH, Kinetics of coagulation factor-x activation by platelet-bound factor ixa, Biochemistry, 29 (1990), pp. 2606–2611, https://doi.org/10. 1021/bi00462a025.
- [20] J. Teruya and V. Kostousov, Antithrombin iii, Medscape, (2020), https://emedicine.medscape.com/

A. WHITESIDE AND E. PHAN

article/2084978-overview#a1.